

## Propanol Amination over Supported Nickel Catalysts: Reaction Mechanism and Role of the Support

Christopher R. Ho, Vincent Defalque, Steven Zheng, and Alexis T. Bell

*ACS Catal.*, **Just Accepted Manuscript** • DOI: 10.1021/acscatal.8b04612 • Publication Date (Web): 21 Feb 2019

Downloaded from <http://pubs.acs.org> on February 21, 2019

### Just Accepted

“Just Accepted” manuscripts have been peer-reviewed and accepted for publication. They are posted online prior to technical editing, formatting for publication and author proofing. The American Chemical Society provides “Just Accepted” as a service to the research community to expedite the dissemination of scientific material as soon as possible after acceptance. “Just Accepted” manuscripts appear in full in PDF format accompanied by an HTML abstract. “Just Accepted” manuscripts have been fully peer reviewed, but should not be considered the official version of record. They are citable by the Digital Object Identifier (DOI®). “Just Accepted” is an optional service offered to authors. Therefore, the “Just Accepted” Web site may not include all articles that will be published in the journal. After a manuscript is technically edited and formatted, it will be removed from the “Just Accepted” Web site and published as an ASAP article. Note that technical editing may introduce minor changes to the manuscript text and/or graphics which could affect content, and all legal disclaimers and ethical guidelines that apply to the journal pertain. ACS cannot be held responsible for errors or consequences arising from the use of information contained in these “Just Accepted” manuscripts.



1  
2  
3  
4  
5  
6  
7  
8  
9  
10  
11  
12 **Propanol Amination over Supported Nickel Catalysts: Reaction Mechanism and**  
13 **Role of the Support**  
14  
15

16  
17 Christopher R. Ho<sup>1,2</sup>, Vincent Defalque<sup>1</sup>, Steven Zheng<sup>1</sup>, Alexis T. Bell<sup>1,2\*</sup>  
18

19 <sup>1</sup>Department of Chemical and Biomolecular Engineering  
20 University of California  
21 Berkeley, CA 94720-1462  
22

23  
24 and  
25

26 <sup>2</sup>Chemical Sciences Division  
27 Lawrence Berkeley National Laboratory  
28 Berkeley, CA 94720  
29  
30

31  
32  
33  
34 Submitted to

35  
36 ACS Catalysis

37  
38 February 21, 2019  
39  
40  
41  
42

43  
44 **\*To whom correspondences should be addressed: [bell@cchem.berkeley.edu](mailto:bell@cchem.berkeley.edu)**  
45  
46  
47  
48  
49  
50  
51  
52  
53  
54  
55

**ABSTRACT**

Ni-supported hydroxyapatite catalyst (Ni/HAP) was characterized and evaluated for propanol amination to propylamine at 423 K. The reaction proceeds via dehydroamination, a process that involves sequential dehydrogenation, condensation, and hydrogenation. Kinetic and isotopic studies indicate that  $\alpha$ -H abstraction from propoxide species limits the rate of the dehydrogenation step, and hence the overall rate of reaction. The rate of propanol dehydrogenation depends on the composition of the support and on the concentration of Ni sites located at the interface between the Ni nanoparticles and the support. Ni/HAP is an order of magnitude more active than Ni/SiO<sub>2</sub> and displays a higher selectivity towards the primary amine. The superior performance of Ni/HAP is attributed to the high density of basic sites on HAP which are responsible for stabilizing alkoxide intermediates and suppressing the disproportionation and secondary amination of amines.

Keywords: hydroxyapatite, HAP, dehydroamination, alkylation, C-N coupling

## INTRODUCTION

Alkylamines are valuable precursors for many rubbers, herbicides, and pharmaceuticals, and are typically produced by the amination of alcohols with ammonia.<sup>1,2</sup> Although this reaction can be performed over solid acid catalysts, the process requires high temperatures (573 – 773 K) and can lead to the formation of unwanted side products, such as olefins.<sup>2,3</sup> An alternative approach is to use a catalyst that dehydrogenates the alcohol to the corresponding alkanal. The alkanal then reacts with ammonia to form the alkylimine which is then hydrogenated to the alkylamine. Suitable catalysts for this approach are Ni, Cu, Co, Pt, and Pd supported on a metal oxide.<sup>4,5,6,7,8,9,10,11,12</sup> These catalysts can operate at lower temperatures (373 – 623 K) due to the higher reactivity of the alkanal compared to the corresponding alcohol. Ni-containing catalysts in particular are promising because they exhibit high activity and stability for a variety of alcohols.<sup>7,13,14,15</sup>

A number of supports for Ni have been investigated for alcohol amination. These include SiO<sub>2</sub>, Al<sub>2</sub>O<sub>3</sub>, CeO<sub>x</sub>, La<sub>2</sub>O<sub>3</sub>, ZrO<sub>2</sub>, TiO<sub>2</sub>, and combinations thereof; however, the role of the support remains unclear.<sup>7,9,11,12,13,14,15,16</sup> Šolcová et al. have evaluated Ni supported on SiO<sub>2</sub>, Al<sub>2</sub>O<sub>3</sub>, ZrO<sub>2</sub>, TiO<sub>2</sub>, and Nb<sub>2</sub>O<sub>5</sub> and found that the rates of diethylene glycol amination to diethylene glycol amine varied only with the number of surface Ni sites, independent of support composition.<sup>15</sup> Based on these results, they concluded that the support affects Ni dispersion but does not play a direct role in the reaction. On the other hand, Shimizu et al. have found that the support has a significant effect on the rate of 2-octanol amination with NH<sub>3</sub>.<sup>7</sup> Of the catalysts tested, Ni/γ-Al<sub>2</sub>O<sub>3</sub> was the most

1  
2  
3 active. However, the reported turnover frequencies were based on the total number of  
4 Ni atoms instead of the number of surface Ni atoms, which makes comparison of the  
5 intrinsic rates unclear. In a later study of 1-octanol amination with aniline over Ni/Al<sub>2</sub>O<sub>3</sub>,  
6 Shimizu et al. determined that the amination rate per surface Ni atom decreases with  
7 increasing Ni particle size, which suggests that Ni atoms located on the corners or  
8 edges of the nanoparticles are more active.<sup>17</sup> Cho et al. have studied 2-propanol  
9 amination with NH<sub>3</sub> over a series of Ni/Al<sub>2</sub>O<sub>3</sub> catalysts with different alumina phases.<sup>18</sup>  
10 They observed that 2-propanol conversion increases with decreasing particle size, even  
11 though no clear trend was found between 2-propanol conversion and Ni surface area.  
12 Large variations in monoisopropylamine selectivity were observed, which was attributed  
13 to differences in Lewis acid site densities of the alumina supports.  
14  
15  
16  
17  
18  
19  
20  
21  
22  
23  
24  
25  
26  
27  
28

29 We have previously shown that hydroxyapatite (HAP) is an active catalyst for the  
30 Guerbet reaction of ethanol, which follows a mechanism similar to that proposed for  
31 alcohol amination.<sup>19</sup> This suggests that HAP would be an excellent support for Ni-  
32 catalyzed amination of alkylamines. The present work was undertaken with the aim of  
33 elucidating the mechanism and kinetics of alcohol amination over Ni/HAP and the role  
34 of the support composition. To this end, we synthesized and characterized Ni/HAP and  
35 compared its activity to Ni/SiO<sub>2</sub> for a series of Ni particle sizes. The results show that for  
36 a given Ni surface area and particle size, Ni/HAP is significantly more active than  
37 Ni/SiO<sub>2</sub>. We propose that the active site is located at the interface between the Ni  
38 nanoparticles and the support. The support does not affect the activation barrier for the  
39 rate-limiting step,  $\alpha$ -H abstraction from a propoxide group, and instead, is responsible  
40 for the formation of surface alkoxides, which are key intermediates in the reaction.  
41  
42  
43  
44  
45  
46  
47  
48  
49  
50  
51  
52  
53  
54  
55

## EXPERIMENTAL METHODS

### Catalyst Synthesis

SiO<sub>2</sub> (Silicycle) and MgO (Sigma-Aldrich) were used without further treatment. Hydroxyapatite (HAP) was synthesized using a modification of the procedure reported by Tsuchida *et al.*<sup>20</sup> and Hanspal *et al.*<sup>21</sup> Aqueous solutions of 0.25 M Ca(NO<sub>3</sub>)<sub>2</sub>•4H<sub>2</sub>O and 0.55 M (NH<sub>4</sub>)<sub>2</sub>HPO<sub>4</sub> were prepared and brought to a pH of 11 by addition of ammonium hydroxide. The calcium solution was added dropwise to the phosphorus solution at room temperature and stirred for 0.5 h before heating to 353 K for an additional 3 h. The resulting slurry was filtered and washed with DI water. γ-Al<sub>2</sub>O<sub>3</sub> was synthesized by calcining boehmite (Süd-Chemie) in 100 mL min<sup>-1</sup> of air at 823 K for 3 h.

Ni-supported catalysts were prepared by incipient wetness impregnation using an aqueous solution of Ni(NO<sub>3</sub>)<sub>2</sub>•6H<sub>2</sub>O on a support that had been dried at 393 K for 1 h. After impregnation, the sample was dried at 298 K overnight and subsequently calcined in 100 mL min<sup>-1</sup> of air at 823 K for 2 h. All Ni-supported catalysts contain 4wt% nickel unless otherwise specified.

Dipropylimine was synthesized by stirring stoichiometric amounts of propanol and propylamine at 298 K. After 5 min, K<sub>2</sub>CO<sub>3</sub> was added to adsorb water and drive the reaction to completion. The product was extracted by centrifugation and stored until later use.

## Characterization Techniques

Powder X-ray diffraction (PXRD) patterns were acquired with a Bruker D8 GADDS diffractometer equipped with a Cu-K $\alpha$  source (40kV, 40mA). BET surface areas were calculated from nitrogen adsorption isotherms obtained using a Micromeritics Gemini VII 2390 surface area analyzer after degassing the catalyst overnight at 393 K. Raman spectra were obtained using a LabRam HR Horiba Jobin Yvon spectrometer equipped with a 532 nm laser. Elemental compositions were measured by Galbraith Laboratories (Knoxville, TN) using ICP-OES.

Ni reducibility was measured by H<sub>2</sub> temperature-programmed reduction (TPR) using a Micromeritics AutoChem II 2920 instrument equipped with a thermal conductivity detector (TCD). Samples were pretreated under He flow at 823 K for 1 h before cooling to 313 K. Catalyst reduction was performed by flowing 4% H<sub>2</sub>/Ar (50 mL min<sup>-1</sup>) and raising the temperature from 313 K to 973 K at 10 K min<sup>-1</sup>. For H<sub>2</sub>-TPR of Ni/HAP, the TCD response due to CO<sub>2</sub> desorption from bulk HAP was corrected for by using the H<sub>2</sub>-TPR spectra of HAP as a reference. Elemental maps of Ni/HAP were obtained using an FEI Quanta FEG 250 scanning electron microscope (SEM) equipped with a Bruker Quantax energy dispersive X-ray spectrometer (EDXS).

Static chemisorption of H<sub>2</sub> was performed using a Micromeritics 3 flex chemisorption analyzer. Samples were evacuated at 383 K for 0.5 h and then reduced in H<sub>2</sub> at the chosen reduction temperature (823 K unless otherwise specified) for 0.5 h. After evacuation at 723 K for 1 h, the samples were cooled to 313 K to measure the adsorption isotherm. Afterwards, the samples were evacuated at 313 K for 1 h and a

1  
2  
3 subsequent isotherm was obtained to quantify the amount of weakly bound H<sub>2</sub>. The total  
4 amount of chemisorbed H<sub>2</sub> was determined by taking the difference between the two  
5 isotherms. O<sub>2</sub> titration was performed by evacuating the same sample at 723 K for 0.5 h  
6 and pulsing in O<sub>2</sub> at 723 K. A Ni site density of 0.0677 nm<sup>2</sup>/atom and adsorption  
7 stoichiometry of 1H:1Ni<sub>surface</sub> were used to calculate the Ni surface area.<sup>22</sup> Average  
8 crystallite size was determined by assuming a spherical crystallite geometry.<sup>22</sup>  
9

### 17 **Measurements of Catalytic Activity**

20  
21 Measurements of reaction rates were carried out using a quartz-tube, packed-  
22 bed reactor (10 mm inner diameter). Quartz wool was placed below the catalyst bed to  
23 hold the catalyst in place. The reactor temperature was maintained using a tube furnace  
24 equipped with a Watlow temperature controller and a K-type thermocouple. Prior to  
25 reaction, the catalyst was treated in 30 mL min<sup>-1</sup> of H<sub>2</sub> at the chosen reduction  
26 temperature (823 K unless otherwise specified) for 0.5 h before cooling to the reaction  
27 temperature.  
28

29  
30 In a typical experiment, propanol was introduced into a stream of He, H<sub>2</sub>, and  
31 NH<sub>3</sub> using a syringe pump (World Precision Instruments, SP100I). Other liquid reactants  
32 were also fed in a similar manner. All experiments were carried out at atmospheric  
33 pressure. Product streams were analyzed by gas chromatography using an Agilent  
34 6890A GC fitted with a HP-5 capillary column (30 m x 0.32 mm x 0.25 μm) and a flame  
35 ionization detector. Measurements of the rate of propanol amination were carried out at  
36 <10% conversion, where the only products observed were propylamine, dipropylamine,  
37 and tripropylamine. The reported amination rates were calculated by assuming that  
38  
39  
40  
41  
42  
43  
44  
45  
46  
47  
48  
49  
50  
51  
52  
53  
54  
55

1  
2  
3 dipropylamine and tripropylamine are formed by amination of two and three equivalents  
4  
5 of propanol, respectively.  
6  
7

## 8 **Theoretical Calculations**

9

10  
11 Calculations of the thermodynamics of selected gas phase reactions were carried  
12  
13 out using the Q-Chem simulation package.<sup>23</sup> Optimization and frequency calculations  
14  
15 were performed at the  $\omega$ B97X-D/6-31G\*\* level of theory while single point calculations  
16  
17 were performed at the  $\omega$ B97X-D/6-311++G(3df,3pd) level of theory.  
18  
19  
20  
21  
22  
23

## 24 **RESULTS AND DISCUSSION**

25

### 26 **Characterization of IE-HAP catalysts**

27

28  
29 The synthesized HAP support has a Ca/P ratio of 1.66 as determined by  
30  
31 elemental analysis, which is consistent with a stoichiometric composition  
32  
33 ( $\text{Ca}_5(\text{PO}_4)_3\text{OH}$ ). The BET surface areas of HAP and Ni/HAP are 91 and 77  $\text{m}^2/\text{g}$ ,  
34  
35 respectively. PXRD patterns for HAP and Ni/HAP are shown in Figure 1. The diffraction  
36  
37 peaks associated with HAP are identical for both samples, indicating that the addition of  
38  
39 nickel does not alter the crystal structure or lattice parameters of HAP. The HAP particle  
40  
41 size is 21 nm for the bare support and 22 nm for Ni/HAP, as estimated by the Scherrer  
42  
43 equation using the (002) diffraction peak. The weak diffraction peaks at  $38^\circ$  and  $42^\circ$  for  
44  
45 Ni/HAP are characteristic of NiO, and the presence of NiO was verified by Raman  
46  
47 spectroscopy (Figure S1). To gauge the reducibility of Ni species on HAP,  $\text{H}_2$ -TPR was  
48  
49 performed (Figure 2). All nickel was fully reduced by 850 K, assuming a 1:1  $\text{H}_2$ :Ni  
50  
51 reduction stoichiometry. The large reduction peak at 590 K corresponds to reduction of  
52  
53  
54  
55  
56  
57  
58  
59  
60

1  
2  
3 bulk NiO species while the shoulder peak at 490 K is due to reduction of very small NiO  
4  
5 particles.<sup>24</sup> The high temperature peak at 750 K is indicative of the reduction of isolated  
6  
7 Ni<sup>2+</sup> species stabilized by the HAP framework, likely due to substitution of two protons or  
8  
9 Ca<sup>2+</sup> in HAP by Ni<sup>2+</sup>.<sup>25</sup>  
10  
11  
12  
13

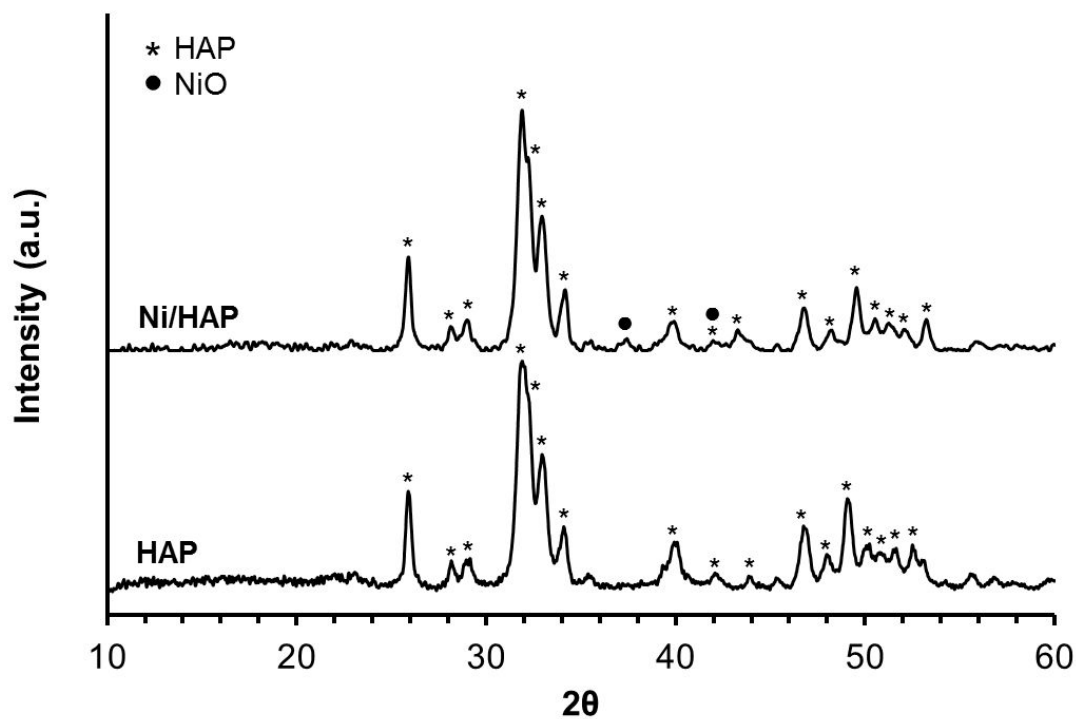


**Figure 1: PXRD spectra of HAP and Ni/HAP**

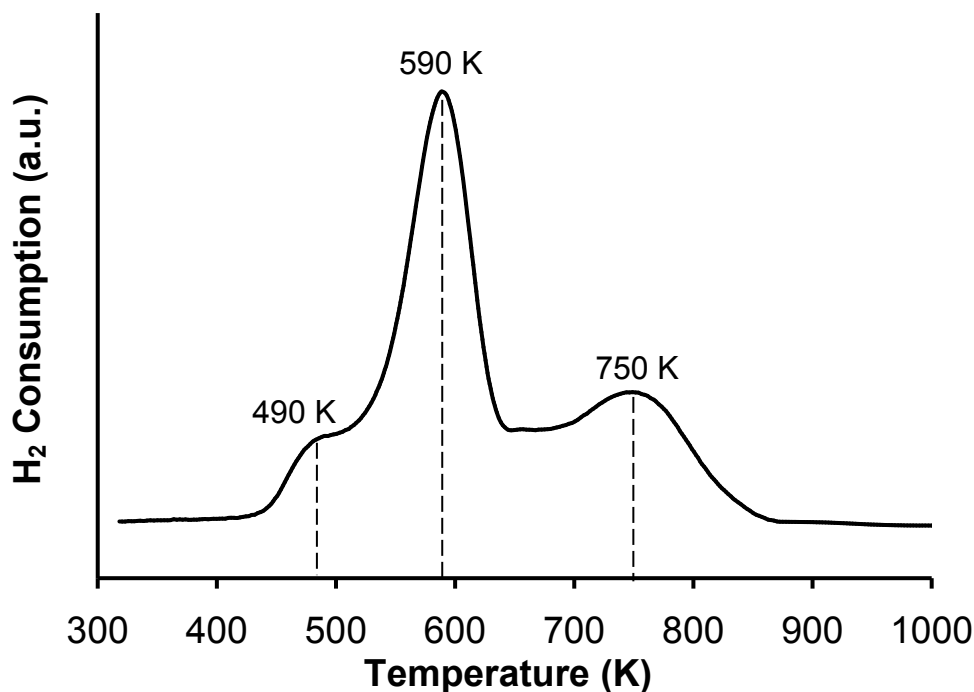
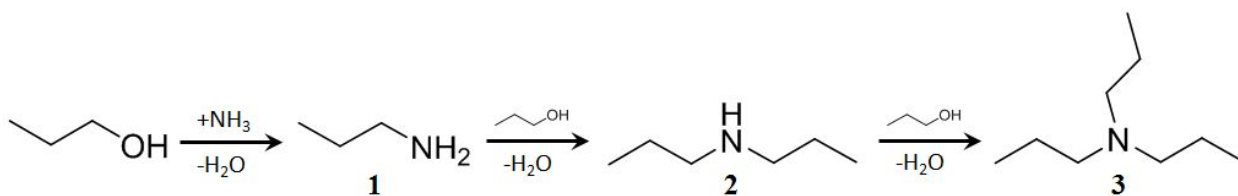


**Figure 2:** H<sub>2</sub>-TPR spectra of Ni/HAP

### Propanol amination over supported Ni catalysts

HAP, Ni/HAP, Ni/SiO<sub>2</sub>, Ni/Al<sub>2</sub>O<sub>3</sub> and Ni/MgO were initially screened for propanol amination at 423 K (Scheme 1). All catalysts except the bare HAP support were active for the reaction, and the only products observed were propylamine **1**, dipropylamine **2**, and tripropylamine **3**. Ni-supported catalysts were inactive without H<sub>2</sub> pretreatment, showing that metallic Ni is necessary for the reaction to proceed. Ni/HAP was the most active catalyst tested, with a propanol conversion of 10.8% (Table 1). Ni/HAP also demonstrated a high selectivity towards propylamine (92%), with the major side product being dipropylamine. Ni/MgO was the least active catalyst with a conversion of 3.3%, while Ni/SiO<sub>2</sub> was the least selective towards propylamine. The differences in conversion and selectivity show that the support composition affects the catalytic activity.



**Scheme 1:** Propanol amination to primary, secondary, and tertiary amines

**Table 1:** Propanol amination with  $\text{NH}_3$  over nickel supported catalysts<sup>[a]</sup>

Catalyst	Ni Particle Size (nm)	Ni Dispersion <sup>[b]</sup>	Ni surface area <sup>[c]</sup> ( $\text{m}^2/\text{g}$ )	Conversion (%)	TOF <sup>[d]</sup> ( $\text{s}^{-1}$ )	Selectivity (%)		
						1	2	3
HAP	-	-	-	~0	-	-	-	-
Ni/HAP	16.5	0.042	3.9	10.8	1.7	92	8	<1
Ni/MgO	10.4	0.014	0.3	3.3	1.1	84	16	<1
Ni/SiO <sub>2</sub>	6.3	0.065	1.6	4.4	0.1	74	24	2
Ni/ $\gamma$ -Al <sub>2</sub> O <sub>3</sub>	4.9	0.041	1.0	4.5	0.2	88	12	<1

[a] Reaction conditions:  $T = 423 \text{ K}$ ; catalyst mass = 0.02 g;  $P_{\text{Propanol}} = 1 \text{ kPa}$ ;  $P_{\text{NH}_3} = 5 \text{ kPa}$ ;  $P_{\text{H}_2} = 95 \text{ kPa}$ ; total gas flow rate at STP =  $30 \text{ mL min}^{-1}$

[b] Dispersion defined as number of surface  $\text{Ni}^0$  atoms over the total loading of Ni

[c] Based on  $\text{H}_2$  chemisorption and  $\text{O}_2$  titration measurements

[d] Turnover frequencies (TOF) defined as rates per perimeter Ni atom as determined by  $\text{H}_2$  chemisorption and  $\text{O}_2$  titration

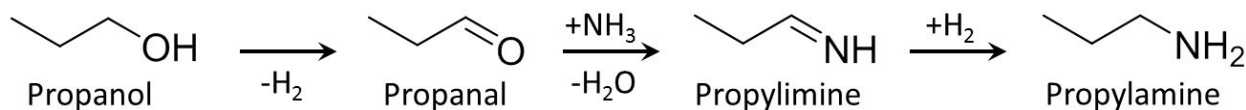
A list of Ni-catalyzed amination rates for aliphatic alcohols have been compiled from literature in Table S3. Direct comparison of rates is difficult since different authors used different reactants and reaction conditions. However, for the reaction of low molecular aliphatic alcohols at similar temperatures, the Ni/HAP catalyst demonstrates a higher TOF than other catalysts reported in literature. We note, however, that Table 1

1  
2  
3 clearly shows that under identical reaction conditions and dispersion of Ni, the TOF for  
4 propanol amination is an order of magnitude higher for Ni/HAP than for Ni/Al<sub>2</sub>O<sub>3</sub>.  
5  
6  
7

### 10 **Mechanism of propanol amination over Ni/HAP**

11  
12 In order to understand the role of the support, it is first necessary to establish the  
13 reaction mechanism of propanol amination over Ni/HAP. Previous studies have shown  
14 that alcohol amination over Ni/SiO<sub>2</sub> and Ni/Al<sub>2</sub>O<sub>3</sub> proceeds via a dehydroamination  
15 pathway, which involves sequential dehydrogenation, C-N coupling, and hydrogenation  
16 steps (Scheme 2).<sup>7,13,26</sup> For aliphatic alcohols, the initial dehydrogenation step has been  
17 reported to be rate-limiting.<sup>4,5</sup> An alternative pathway involves direct coupling of alcohol  
18 and ammonia in one step, which occurs over solid acid catalysts such as zeolites.<sup>27</sup>  
19 One key difference between the two pathways is that hydroamination requires an  
20 alcohol reactant with an  $\alpha$ -H for the initial dehydrogenation step. To determine which  
21 pathway occurs over Ni/HAP, the amination of tert-butanol was investigated. Prior work  
22 has shown that tert-butanol will readily couple with NH<sub>3</sub> via direct amination but cannot  
23 occur through dehydroamination because tert-butanol lacks an  $\alpha$ -proton necessary to  
24 undergo dehydrogenation.<sup>27</sup> When tert-butanol and NH<sub>3</sub> were fed over 4%Ni/HAP at  
25 423 K under flowing H<sub>2</sub>, no products were formed (Table S1), suggesting that direct  
26 amination does not occur over Ni/HAP. The mechanism was further probed by feeding  
27 NH<sub>3</sub> and H<sub>2</sub> with propanal, which is an intermediate in the dehydroamination pathway.  
28 Propanal converted quantitatively to propylamine (Table S1), indicating that the  
29 amination of propanol follows a dehydroamination pathway. Moreover, the rapid rate of  
30  
31  
32  
33  
34  
35  
36  
37  
38  
39  
40  
41  
42  
43  
44  
45  
46  
47  
48  
49  
50  
51  
52  
53  
54  
55  
56  
57  
58  
59  
60

propanol conversion indicates that the initial dehydrogenation step is slow, consistent with previous literature reports for Ni-supported catalysts.<sup>17</sup>

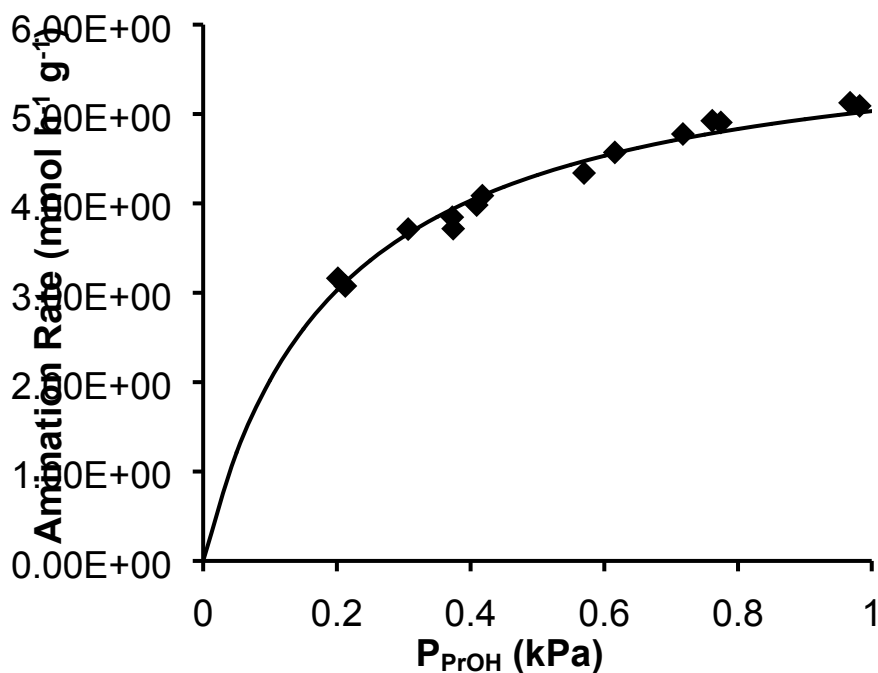


**Scheme 2:** Hydroamination pathway for propanol amination to propylamine

Kinetic isotope experiments with ethanol were performed to verify the pathway and shed more light on the reaction mechanism. The rate of reaction was unaffected when H<sub>2</sub>/ethanol was replaced with D<sub>2</sub>/ethanol-D1 (Table S2), showing that the dissociation of H<sub>2</sub> and cleavage of the O-H bond in propanol are not rate-limiting. However, a kinetic isotope effect (KIE) was observed when D<sub>2</sub>/ethanol-D6 was used ( $k_H/k_D=1.5$ ). This result is in agreement with prior studies suggesting that  $\alpha$ -H abstraction is rate-limiting in the dehydrogenation step. The magnitude of the KIE is similar to what Baiker et al. have reported for octanol amination over Cu/Al<sub>2</sub>O<sub>3</sub>.<sup>5</sup>

The dependences of the rate propanol amination on reactant partial pressures are shown in Figures 3 and 4. The amination rate is positive order with respect to propanol at low propanol partial pressures and approaches zero order with increasing propanol partial pressures for the range of partial pressures tested ( $P_{PrOH} = 0.2-1.0$  kPa). In contrast, the rate is zero order with respect to NH<sub>3</sub> for all NH<sub>3</sub> partial pressures tested (3.4-16.8 kPa). The results suggest that the sites responsible for propanol dehydrogenation are predominantly empty or are occupied by propanol-derived species. NH<sub>3</sub> has been proposed to aid in alcohol dehydrogenation over a Ni(111) surface.<sup>28</sup>

1  
2  
3 However, the rate over Ni/HAP does not vary with  $\text{NH}_3$  partial pressure. Thus, an  $\text{NH}_3$ -  
4 mediated pathway may not be relevant for supported Ni catalysts.  
5  
6



30  
31 **Figure 3:** Effect of propanol partial pressure on amination rate. Reaction conditions:  $T =$   
32  $423 \text{ K}$ ;  $\text{Ni/HAP} = 0.02 \text{ g}$ ;  $P_{\text{NH}_3} = 5 \text{ kPa}$ ;  $P_{\text{H}_2} = 95 \text{ kPa}$ ; total gas flow rate at STP =  $60 \text{ mL}$   
33  $\text{min}^{-1}$ .  
34  
35  
36  
37  
38  
39  
40  
41  
42  
43  
44  
45  
46  
47  
48  
49  
50  
51  
52  
53  
54  
55

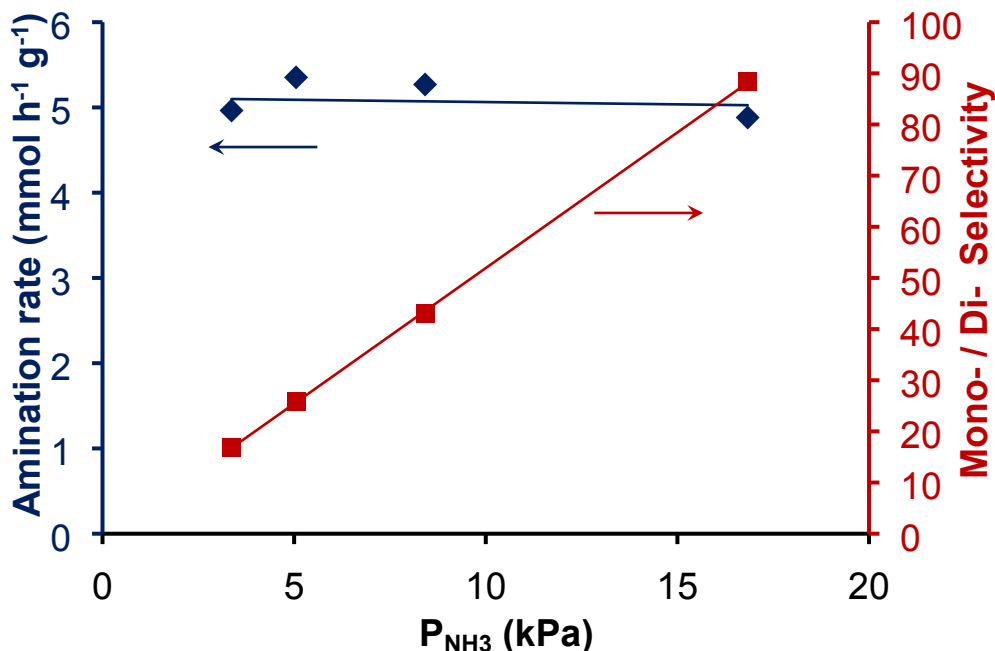


**Figure 4:** Effect of  $\text{NH}_3$  partial pressure on propanol amination rate and selectivity of propylamine vs. dipropylamine. Reaction conditions:  $T = 423 \text{ K}$ ;  $\text{Ni}/\text{HAP} = 0.01 \text{ g}$ ;  $P_{\text{Propanol}} = 1 \text{ kPa}$ ;  $P_{\text{H}_2} = 83\text{-}96 \text{ kPa}$ ; total gas flow rate at STP =  $30 \text{ mL min}^{-1}$ .

As seen in Figure 4, the ratio of the production of propylamine to dipropylamine shows a strong dependence on  $\text{NH}_3$  partial pressure. This finding is consistent with the proposed mechanism in which a propanal intermediate can react with either  $\text{NH}_3$  to form propylamine or with propylamine to form dipropylamine. One interesting question is whether C-N bond formation takes place in the gas phase or on the surface. Several groups have reported that the C-N coupling reaction in the liquid phase is facile and can occur spontaneously in solution, while others have hypothesized that the reaction takes place on the catalyst surface based on the observation of a dependence of the product selectivity on catalyst composition.<sup>29,30</sup> To probe for C-N coupling in the gas phase, propanal and propylamine were fed through a blank reactor. Quantitative conversion to

1  
2  
3 dipropylimine was observed, showing that the reaction does not require a catalyst  
4 (Table S1). However, when a similar experiment was conducted with propanal and  
5 ammonia, no products were formed (Table S1). Primary imines are known to be  
6 unstable, so the lack of reaction could be due to the inherent thermodynamics instead of  
7 a kinetic limitation. Gas phase DFT calculations reveal that the Gibbs free energy of  
8 reaction,  $\Delta G_{\text{rxn}}$ , for propanal and  $\text{NH}_3$  to form propylimine is +33 kJ/mol while the  $\Delta G_{\text{rxn}}$   
9 for the reaction of propanal and propylamine to form dipropylimine is -0.6 kJ/mol  
10 (Scheme S1). The subsequent hydrogenation of propylimine ( $\Delta G_{\text{rxn}} = -62$  kJ/mol) or  
11 dipropylimine ( $\Delta G_{\text{rxn}} = -39$  kJ/mol) are both highly favorable. Based on these Gibbs free  
12 energy calculations, the equilibrium conversion of propanal and  $\text{NH}_3$  to propylimine is  
13 approximately 1%. It is therefore tempting to suggest that coupling of propanal and  $\text{NH}_3$   
14 requires a catalyst, since no propylimine was detected in the product stream. However,  
15 we cannot rule out the possibility that small amounts of propylimine are formed but  
16 hidden beneath the propanal signal in the chromatogram, since the retention time of  
17 propylimine could only be estimated due to lack of a stable propylimine standard.

18  
19 The amination rate and product selectivity are invariant with  $\text{H}_2$  partial pressure  
20 for  $P_{\text{H}_2} = 5\text{-}95$  kPa (Figure S2). However the catalyst quickly deactivates if  $\text{H}_2$  is not  
21 present due to the formation of metal nitrides and carbonaceous species.<sup>8,11,31</sup> Although  
22  $\text{H}_2$  does not play a direct role in the dehydrogenation reaction, a small amount is  
23 necessary to keep the Ni nanoparticles in their active metallic state. Possible product  
24 inhibition was investigated by co-feeding  $\text{H}_2\text{O}$ , butanal (as a proxy for propanal),  
25 diethylamine (as a proxy for dipropylamine), or triethylamine (as a proxy for  
26 tripropylamine). In all cases, no significant change in reaction rate was observed,

1  
2  
3 indicating that none of the above products or intermediates compete with propanol for  
4 the active site. (Figure S3).  
5  
6

### 7 **Role of support in propanol amination over Ni catalysts**

8  
9  
10 To gain more insight into the site requirements and role of the support, a series  
11 of Ni/HAP and Ni/SiO<sub>2</sub> catalysts with different Ni particle sizes were synthesized by  
12 varying the metal loading and reduction temperature (Table 2). Larger Ni particles were  
13 obtained at higher Ni loadings and higher reduction temperatures. Propanol amination  
14 rates were measured for all catalysts and are shown in Figure 5. When the rates are  
15 normalized by the number of surface Ni atoms, the rates decrease with increasing Ni  
16 particle size, suggesting that the Ni atoms located at the edges or corners are the active  
17 sites. Shimizu et al. have reported a similar observation for cyclodecanol  
18 dehydrogenation over Ni/θ-Al<sub>2</sub>O<sub>3</sub>.<sup>32</sup> An alternative hypothesis is that the support plays a  
19 direct role in alcohol dehydrogenation, in which case the active sites would be Ni  
20 perimeter sites located at the interface of the metal and the support. This would explain  
21 why Ni/HAP is more active than Ni/SiO<sub>2</sub> for a given particle size. The number of  
22 perimeter Ni particles were determined by assuming the Ni nanoparticle has the shape  
23 of a truncated cuboctahedron and then calculating the number of perimeter sites based  
24 on the nanoparticle size and number of Ni surface sites, as demonstrated by Cargnello  
25 et al.<sup>33</sup> Note that since particle surface area is proportional to the square of a  
26 characteristic radius, and particle perimeter is proportional to its radius, the relationship  
27 between perimeter sites, surface sites, and particle size should be similar for various  
28 particle geometries. When the rates are normalized by the number of perimeter Ni sites  
29  
30  
31  
32  
33  
34  
35  
36  
37  
38  
39  
40  
41  
42  
43  
44  
45  
46  
47  
48  
49  
50  
51  
52  
53  
54  
55  
56  
57  
58  
59  
60

(Figure 5b), the turnover frequencies become invariant with particle size, suggesting that the Ni perimeter sites are the ones active for propanol dehydrogenation.

**Table 2:** Synthesis conditions and characterization of Ni/HAP and Ni/SiO<sub>2</sub> catalysts

Catalyst	Ni loading <sup>[a]</sup> (wt %)	Reduction temperature (K)	Ni surface area <sup>[b]</sup> (m <sup>2</sup> /g)	Fraction of Ni reduced <sup>[b]</sup> (%)	Ni particle size <sup>[a]</sup> (nm)
Ni/HAP-8.3	4.02	623	2.2	69	8.3
Ni/HAP-9.9	4.02	673	2.3	82	9.9
Ni/HAP-13.0	4.02	723	2.0	95	13.0
Ni/HAP-16.5 (Ni/HAP)	4.02	823	1.6	99	16.5
Ni/SiO <sub>2</sub> -6.3 (Ni/SiO <sub>2</sub> )	3.95	823	3.9	93	6.3
Ni/SiO <sub>2</sub> -7.6	3.95	923	3.4	97	7.6
Ni/SiO <sub>2</sub> -12.5	11.3	823	6.7	98	12.5
Ni/SiO <sub>2</sub> -16.6	22.9	823	8.8	94	16.6

[a] From ICP-OES conducted by Galbraith Laboratories

[b] Based on H<sub>2</sub> chemisorption and O<sub>2</sub> titration measurements

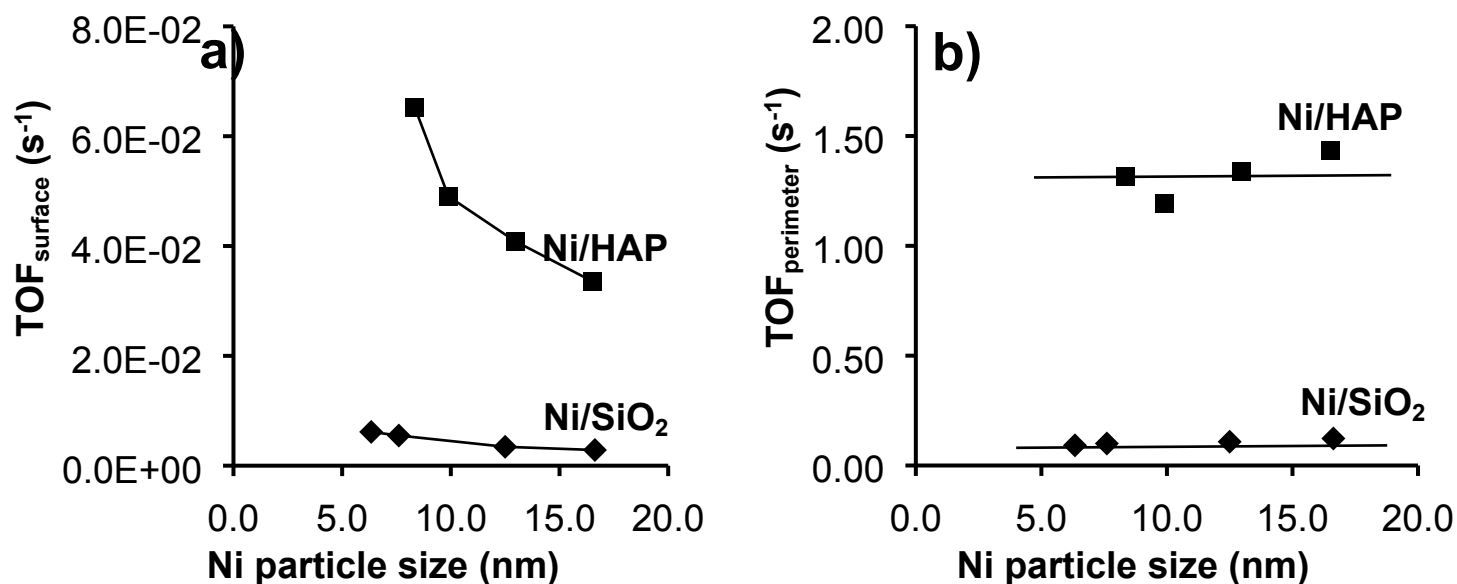
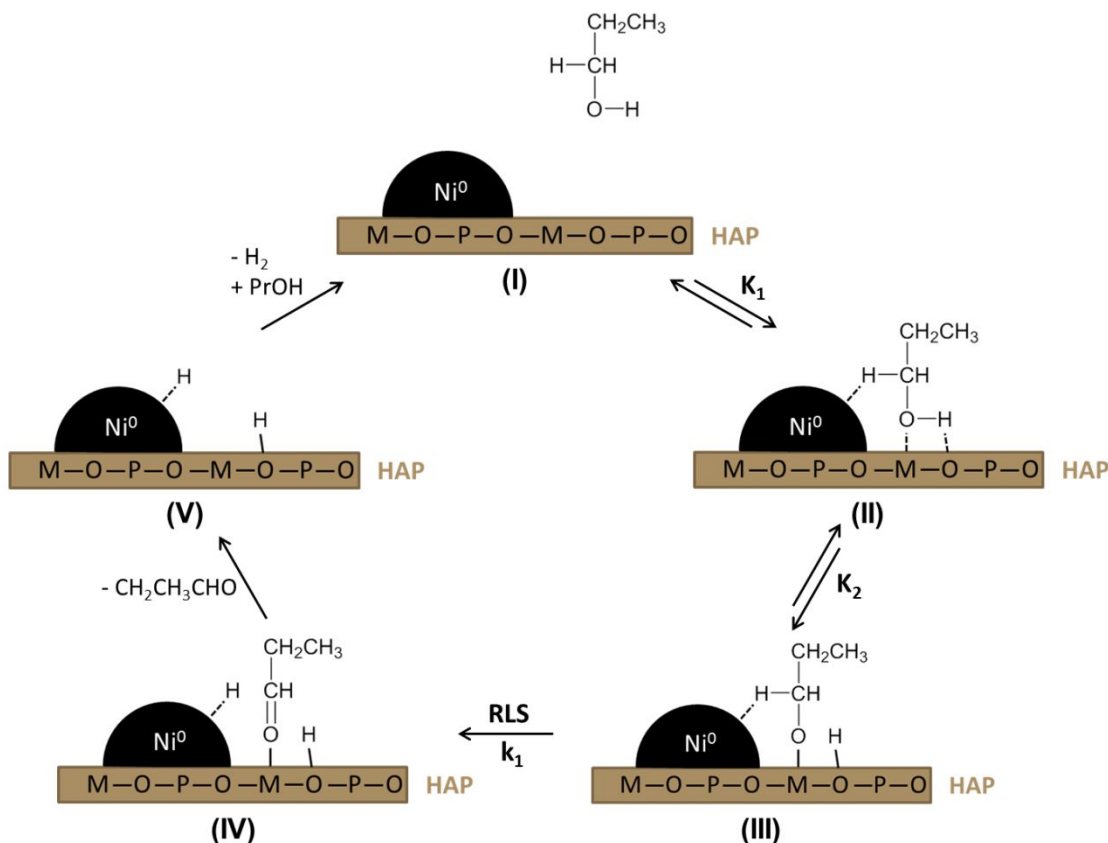


**Figure 5:** Effect of support and Ni particle size on turnover frequencies (TOF) of propanol amination. a) TOF is based on the number of surface Ni sites. b) TOF is based on the number of perimeter Ni sites. Reaction conditions: T = 423 K; mass<sub>catalyst</sub> = 0.02 g; P<sub>Propanol</sub> = 1 kPa; P<sub>NH<sub>3</sub></sub> = 5 kPa; P<sub>H<sub>2</sub></sub> = 95 kPa; total gas flow rate at STP = 60 mL min<sup>-1</sup>.

To determine why the support affects reaction rates, it is helpful to construct a plausible mechanism for propanol dehydrogenation over Ni/HAP (Scheme 3). The adsorption of propanol and formation of the corresponding propoxide are facile over HAP, suggesting that gas phase propanol (I), molecularly adsorbed propanol (II), and surface propoxide (III) are in pseudo-equilibrium with each other.<sup>34</sup> The subsequent rate-limiting  $\alpha$ -H abstraction occurs on a neighboring Ni site (IV), since dehydrogenation does not proceed in the absence of Ni at 423 K. Recombination of the surface hydrogen atoms (V) and desorption of the products complete the catalytic cycle.



**Scheme 3:** Proposed reaction mechanism for propanol dehydrogenation over Ni/HAP

An alternative mechanism is that dehydrogenation takes place exclusively on Ni, and the support only serves to modify the electronic properties of the metal. In this case, the activation barrier for  $\alpha$ -H abstraction would depend on the nature of the support. To test this possibility, the activation energy was measured over Ni/HAP-16.5 and Ni/SiO<sub>2</sub>-12.5 at  $P_{\text{PrOH}} = 2.0$  kPa, where all interfacial sites are covered predominantly with propanol derived surface species (Figures S4, S5). As shown in Figure 6, The activation energies over both catalysts are similar ( $E_{a, \text{Ni/HAP}} = 68$  kJ/mol;  $E_{a, \text{Ni/SiO}_2} = 70$  kJ/mol), indicating that the support does not affect the electronic properties of the Ni

1  
2  
3 nanoparticles and, hence, the rate of the  $\alpha$ -H abstraction step. Instead, the difference in  
4  
5 turnover frequencies between Ni/HAP and Ni/SiO<sub>2</sub> suggest that the properties of the  
6  
7 support affect the concentration of the active surface propoxide species. Several groups  
8  
9 have shown that alcohol adsorption on SiO<sub>2</sub> leads mainly to molecularly adsorbed  
10  
11 alcohol, and only a small fraction of surface species are alkoxides which form by  
12  
13 condensation of alcohol/silanol groups or opening of the siloxane bridges.<sup>35,36,37</sup> On the  
14  
15 other hand, HAP is known to have a high density of basic sites that can activate  
16  
17 alcohols.<sup>21,38</sup> This is evident when looking at adsorption microcalorimetry of ethanol.  
18  
19 The differential heat of ethanol adsorption over HAP ( $\Delta H_{\text{EtOH}} \approx 100$  kJ/mol) remains  
20  
21 constant up to a surface coverage of 4  $\mu\text{mol m}^{-2}$ , which is indicative of a surface that  
22  
23 contains strongly chemisorbed ethanol species.<sup>21</sup> For SiO<sub>2</sub>, the differential heat of  
24  
25 ethanol adsorption decreases rapidly from  $\sim 100$  kJ/mol to  $\sim 60$  kJ/mol as the surface  
26  
27 coverage increases to 1  $\mu\text{mol m}^{-2}$ , consistent with the idea that most alcohols on SiO<sub>2</sub>  
28  
29 are weakly bound, physisorbed species.<sup>35</sup> Shimuzu et al. have proposed a similar role  
30  
31 for the support in 2-propanol dehydrogenation over Ni/Al<sub>2</sub>O<sub>3</sub>.<sup>32</sup> Based on catalyst  
32  
33 screening and FTIR studies, the group hypothesized that the basic sites in  $\theta$ -Al<sub>2</sub>O<sub>3</sub> were  
34  
35 responsible for the formation of 2-propoxide species.<sup>32</sup> This conclusion parallels that  
36  
37 drawn from studies of alcohol amination carried out with homogenous catalysts, in  
38  
39 which alcohol dehydrogenation and amination over metal complexes typically require  
40  
41 the addition of a base such as K<sub>2</sub>CO<sub>3</sub> to deprotonate the alcohol and form the  
42  
43 alkoxide.<sup>39,40</sup> Although MgO is a basic support that can catalyze alkoxide formation, the  
44  
45 Ni/MgO catalyst exhibited a lower TOF than Ni/HAP (Table 1). This is likely due to the  
46  
47 higher density of base sites on the HAP support, which translates to a higher  
48  
49  
50  
51  
52  
53  
54  
55

concentration of propoxide species on the surface, and hence, to a higher TOF even after normalizing rates per perimeter Ni atom.<sup>21</sup>

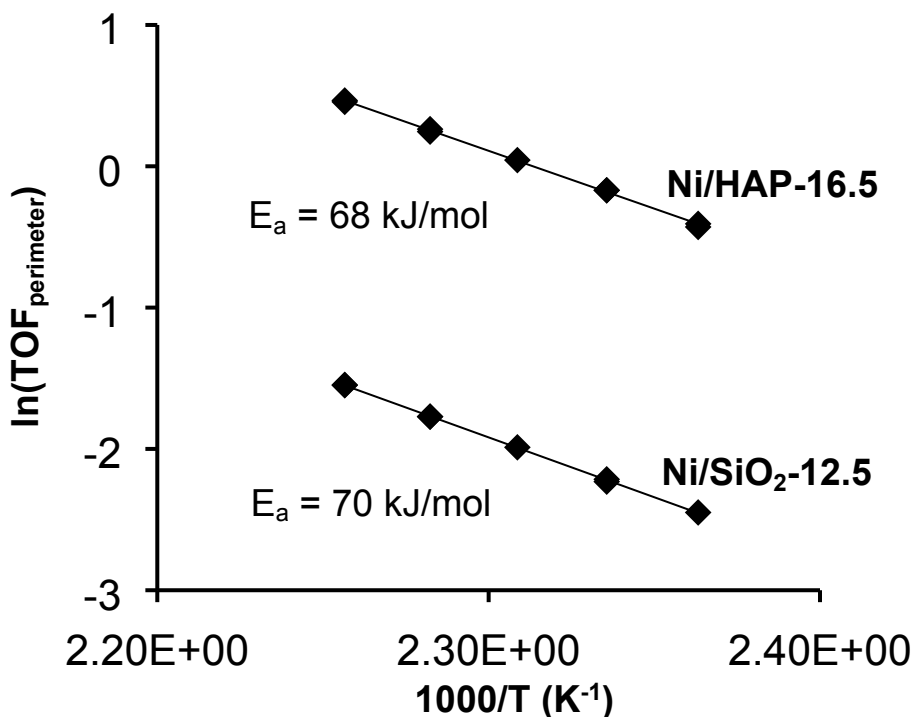


**Figure 6:** Arrhenius plots of propanol amination over Ni/HAP-16.5 and Ni/SiO<sub>2</sub>-12.5. Reaction conditions: T = 423 K; mass<sub>catalyst</sub> = 0.02 g; P<sub>Propanol</sub> = 1 kPa; P<sub>NH<sub>3</sub></sub> = 5 kPa; P<sub>H<sub>2</sub></sub> = 95 kPa; total gas flow rate at STP = 60 mL min<sup>-1</sup>.

An additional factor that could explain the large difference in activity between Ni/HAP and Ni/SiO<sub>2</sub> is the ability of Ni/HAP to catalyze hydrogen transfer reactions, since HAP is known to be active for hydrogen transfer reactions between alcohols and aldehydes.<sup>19,41,42,43</sup> These hydrogen transfer reactions are rapid in comparison to dehydrogenation and can accelerate condensation rates by providing an alternate pathway for producing aldehydes.<sup>19</sup> To determine whether Ni/HAP is active for hydrogen transfer between alcohols and imines, propanol and dipropylimine were fed to

1  
2  
3 the reactor. No dipropylamine was observed in the product stream, indicating that  
4  
5 hydrogen transfer to a C=N bond is much more difficult than the corresponding reaction  
6  
7 over the more polar C=O bond.  
8  
9

10  
11 Space time studies over Ni/HAP and Ni/SiO<sub>2</sub> were performed to evaluate the  
12  
13 effect of support on product selectivity. For both catalysts, propylamine selectivity  
14  
15 decreased and dipropylamine selectivity increased with increasing propanol conversion,  
16  
17 as shown in Figure 7. This is consistent with a mechanism in which propylamine is a  
18  
19 primary product that can react further to form dipropylamine. There are two main  
20  
21 pathways for dipropylamine formation. One pathway is a consecutive amination  
22  
23 reaction, wherein propylamine and propanol react to give dipropylamine and water. The  
24  
25 other pathway is the disproportionation of two equivalents of propylamine to give  
26  
27 dipropylamine and NH<sub>3</sub>. For a given propanol conversion, Ni/HAP is more selective  
28  
29 towards propylamine than Ni/SiO<sub>2</sub>.  
30  
31  
32  
33  
34  
35  
36  
37  
38  
39  
40  
41  
42  
43  
44  
45  
46  
47  
48  
49  
50  
51  
52  
53  
54  
55  
56  
57  
58  
59  
60

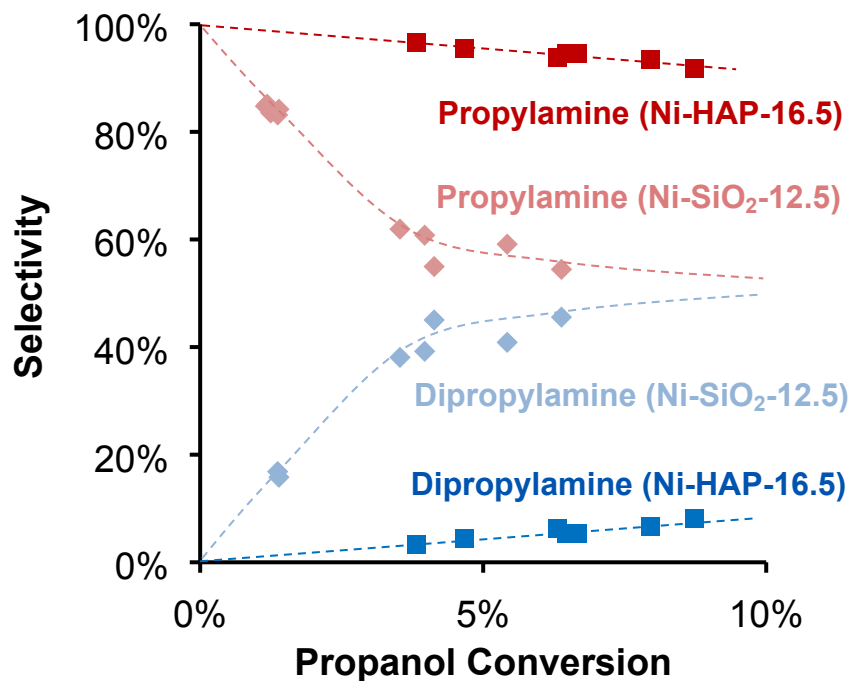
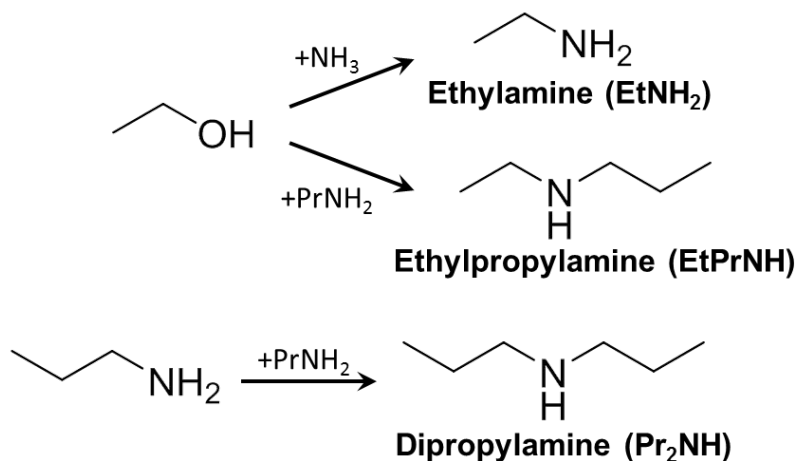


**Figure 7:** Spacetime studies showing how the selectivity of propylamine and dipropylamine as a function of propanol conversion over Ni/HAP-16.5 and Ni/SiO<sub>2</sub>-12.5. Reaction conditions: T = 423 K; mass<sub>catalyst</sub> = 0.02 g; P<sub>Propanol</sub> = 1 kPa; P<sub>NH<sub>3</sub></sub> = 5 kPa; P<sub>H<sub>2</sub></sub> = 95 kPa.

To determine whether this difference in selectivity is due to differences in secondary amination or disproportionation rates, experiments with ethanol/NH<sub>3</sub>/propylamine feeds were performed to decouple the amination and disproportionation rates. Primary amination of ethanol yields ethylamine, secondary amination of ethanol yields ethylpropylamine, and disproportionation of propylamine yields dipropylamine (Scheme 4). The disproportionation rate was three times higher over Ni/SiO<sub>2</sub> compared to Ni/HAP, which partly explains why Ni/HAP is more selective for the primary amine than Ni/SiO<sub>2</sub> (Table 3). The reason for the low disproportionation rates over Ni/HAP is likely due to a lack of strong Lewis acid sites, which are known to be active for disproportionation.<sup>31</sup> The

1  
2  
3 small fraction of unreduced Ni in Ni/SiO<sub>2</sub> can lead to the generation of Lewis acid sites,  
4  
5 and Verhaak et al. have demonstrated that Ni/SiO<sub>2</sub> is an active catalyst for  
6  
7  
8 disproportionation.<sup>31</sup>  
9  
10  
11  
12  
13



**Scheme 4:** Possible amination and disproportionation reactions for an ethanol/NH<sub>3</sub>/propylamine feed

**Table 3:** Disproportionation of propylamine over Ni/HAP-16.5 and Ni/SiO<sub>2</sub>-12.5. Reaction conditions: T = 423 K; mass<sub>catalyst</sub> = 0.01 g; P<sub>PrOH</sub> = 0.1 kPa; P<sub>Ethylamine</sub> = 0.1 kPa; P<sub>NH3</sub> = 5 kPa; P<sub>H2</sub> = 95 kPa; total gas flow rate at STP = 30 mL min<sup>-1</sup>.

41  
42  
43  
44  
45  
46  
47  
48  
49  
50  
51  
52  
53  
54  
55  
56  
57  
58  
59  
60

Catalyst	Formation rate (mmol h <sup>-1</sup> g <sub>cat</sub> <sup>-1</sup> )		
	Ethylamine	Ethylpropylamine	Dipropylamine
Ni/HAP-16.5	1.90	1.39	0.62
Ni/SiO <sub>2</sub> -12.5	0.69	1.50	1.79

The relative rates of primary and secondary amination also depend on the support. Ethylamine and ethylpropylamine are both formed from a common ethanal intermediate, and the ratio of their formation rates is proportional to the ratio of  $\text{NH}_3$  and propylamine partial pressures. This is illustrated in eq 1, where  $k$  represents a rate constant,  $P$  represents the partial pressure, and  $[\text{CH}_3\text{CHO}^*]$  represents the surface concentration of propanal on the support. This expression is consistent with the observed trends in product selectivities and in the  $\text{NH}_3$  kinetics of propanol amination (Figure 4).

$$\frac{r_{\text{EtNH}_2}}{r_{\text{EtPrNH}}} = \frac{k_{\text{EtNH}_2} P_{\text{EtNH}_2} [\text{CH}_3\text{CHO}^*]}{k_{\text{EtPrNH}} P_{\text{EtPrNH}} [\text{CH}_3\text{CHO}^*]} \quad (1)$$

Coupling of ethanal is more facile with propylamine than with  $\text{NH}_3$  since propylamine is a stronger nucleophile and secondary imines are more stable than primary imines. The ratio of rate constants for ethanal coupling with propylamine vs  $\text{NH}_3$   $\left(\frac{k_{\text{EtPrNH}}}{k_{\text{EtNH}_2}}\right)$  is 37 over Ni/HAP and 109 over Ni/ $\text{SiO}_2$ . The different rate constants for the two catalysts indicate that the support plays an important role in the condensation step. Furthermore, this is evidence that C-N coupling occurs on the support surface and not exclusively in the gas-phase. We hypothesize that  $\frac{k_{\text{EtPrNH}}}{k_{\text{EtNH}_2}}$  is higher over Ni/HAP because of the basic nature of the HAP support, which lowers the effective concentration of adsorbed propylamine compared to  $\text{SiO}_2$ . Thus, Ni/HAP is more selective towards the primary amine than Ni/ $\text{SiO}_2$  because both the secondary amination and disproportionation reactions are suppressed more greatly over HAP.

1  
2  
3 One question that arises is whether the density of active Ni sites affects the  
4 product selectivity. Propanol amination with propylamine has the same mechanism and  
5 site requirements as propanol amination with  $\text{NH}_3$ , so the number of active Ni sites  
6 should not affect the relative selectivity of these two reactions, as long as results are  
7 compared at isoconversion. However, the density of active Ni sites could affect the  
8 relative rate of amination and disproportionation.  
9  
10  
11  
12  
13  
14  
15  
16

17 While a detailed mechanistic understanding of amine disproportionation is  
18 outside the scope of this work, it has been generally proposed that disproportionation  
19 occurs in a 3-step process that involves dehydrogenation of the propylamine to  
20 propylimine, coupling of propylimine with another propylamine, and hydrogenation of the  
21 resulting secondary imine to form dipropylamine.<sup>4,31</sup> Starting from a propylimine  
22 intermediate, hydrogenation would yield propylamine, while disproportionation would  
23 yield dipropylamine. Thus, the density of active Ni sites could affect the rate of  
24 propylimine hydrogenation, which would impact product selectivity.  
25  
26  
27  
28  
29  
30  
31  
32  
33  
34  
35  
36

37 To investigate this possibility, the selectivity to propylamine at a given propanol  
38 conversion (~10% for Ni/HAP, ~3.5% for Ni/SiO<sub>2</sub>) was plotted as a function of the  
39 number of Ni perimeter sites for all supported Ni catalysts (Figure S7). The selectivity to  
40 propylamine appears to be invariant with the number of perimeter Ni sites for a given  
41 support. To explain this result, we note that disproportionation of propylamine occurs  
42 under reaction conditions (Table 3), indicating that propylamine dehydrogenation to  
43 propylimine is a relevant process. Thus, increasing the density of Ni sites will increase  
44 both the rate of propylimine hydrogenation and propylamine dehydrogenation, which  
45  
46  
47  
48  
49  
50  
51  
52  
53  
54  
55

1  
2  
3 would explain why the density of Ni perimeter sites does not significantly affect product  
4 selectivity (Scheme S2).  
5  
6

7  
8  
9 However, for a catalyst with a low density of active Ni sites, increasing the  
10 number of Ni sites could lead to an increase in selectivity. For example, the basic  
11 4%Ni/MgO exhibits a lower selectivity to propylamine compared to the acidic  
12 4%Ni/Al<sub>2</sub>O<sub>3</sub>. This appears to contradict the idea that Lewis acidic supports are more  
13 active for disproportionation and secondary amination. However, close inspection of the  
14 4%Ni/MgO catalyst reveals that only 14% of Ni is reduced after treatment in H<sub>2</sub> at 773  
15 K. This is due to the difficulty of reducing Ni on a MgO support. The 4%Ni/MgO catalyst  
16 has fewer active Ni sites compared to 4%Ni/Al<sub>2</sub>O<sub>3</sub> (0.3 vs 2.2 μmol/g<sub>cat</sub>). In addition, the  
17 unreduced NiO on MgO can serve as Lewis acid sites. These two factors could explain  
18 why Ni/MgO has a lower selectivity to propylamine than 4%Ni/Al<sub>2</sub>O<sub>3</sub>.  
19  
20  
21  
22  
23  
24  
25  
26  
27  
28  
29  
30  
31

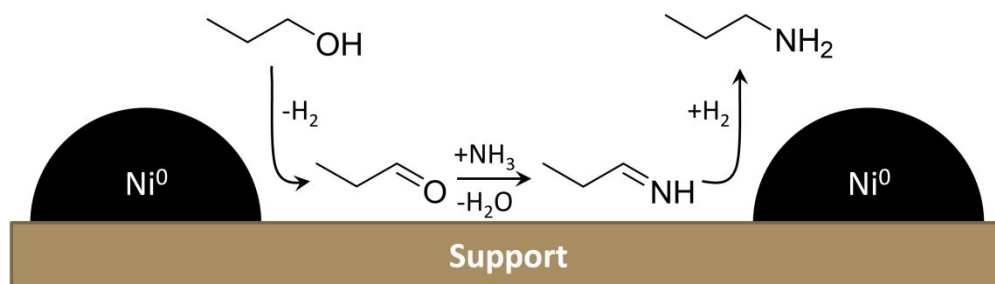
32 To test this hypothesis, a 12%Ni/MgO catalyst was synthesized by an  
33 impregnation method. Compared to 4%Ni/MgO, the 12%Ni/MgO catalyst has a higher  
34 Ni loading and larger NiO particles, which results in a higher fraction of reduced Ni after  
35 H<sub>2</sub> treatment. As a result, the 12%Ni/MgO catalyst has more active Ni sites and fewer  
36 Lewis acid sites than 4%Ni/MgO, which should lead to an increase in propylamine  
37 selectivity. Indeed, at a conversion of ~3.5%, the propylamine selectivity over the  
38 12%Ni/MgO (89%, Table S1) was higher than that of 4%Ni/MgO (84%). Thus,  
39 propylamine selectivity can be improved by increasing the number of Ni sites and  
40 decreasing the number of Lewis acid sites. Unfortunately, the contribution due to the  
41 two effects could not be decoupled. A similar trend has been observed by Cabello et al.  
42  
43  
44  
45  
46  
47  
48  
49  
50  
51  
52  
53  
54  
55

1  
2  
3 over Ni/hydrotalcite, where the Ni reducibility and support basicity depend on the Ni and  
4 Mg loadings.<sup>44</sup> For a more comprehensive review of support effects on selectivity, the  
5 authors refer Gomez et al.<sup>30</sup>  
6  
7  
8  
9  
10

## 11 12 13 14 **CONCLUSIONS**

15  
16  
17 We have demonstrated that Ni/HAP is an active catalyst for propanol amination  
18 to propylamine. The reaction proceeds through a dehydroamination pathway and is  
19 limited by the rate of  $\alpha$ -H abstraction from propanol. The turnover frequency for this  
20 reaction is invariant with Ni particle size when normalized by the number of perimeter Ni  
21 atoms, suggesting that the active sites for dehydrogenation are located at the interface  
22 between the metal and the support. Ni/HAP is more active and selective towards the  
23 primary amine than Ni/SiO<sub>2</sub>, highlighting the importance of the support. Although Ni is  
24 solely responsible for the  $\alpha$ -H abstraction step, the support affects the reaction rate by  
25 deprotonating the alcohol to form active alkoxide intermediates. The subsequent  
26 coupling of propanal with ammonia is rapid and quantitative, independent of the  
27 ammonia partial pressure. While propylimine formed by this reaction is  
28 thermodynamically unstable, its rapid hydrogenation over the Ni nanoparticles leads to  
29 the thermodynamically favorable formation of propylamine. Experimental evidence  
30 suggests that the reaction of propanal with ammonia occurs on the surface of HAP,  
31 whereas the hydrogenation of propylimine occurs on the surface of the Ni nanoparticles  
32 (Scheme 5). The secondary reaction of product propylamine with propanal to form  
33 dipropylamine also occurs on the surface of HAP but is increasingly suppressed as the  
34  
35  
36  
37  
38  
39  
40  
41  
42  
43  
44  
45  
46  
47  
48  
49  
50  
51  
52  
53  
54  
55

1  
2  
3 partial pressure of ammonia is increased. This secondary reaction occurs to a much  
4  
5 lower degree over Ni/HAP than Ni/SiO<sub>2</sub>. Finally, we have found that the  
6  
7 disproportionation of propylamine to dipropylamine and ammonia is disfavored over  
8  
9 Ni/HAP compared to Ni/SiO<sub>2</sub>.



24 **Scheme 5:** Proposed reaction mechanism for propanol amination over Ni/HAP

## 25 26 27 28 29 **SUPPORTING INFORMATION**

30  
31  
32 Raman spectra and EDX analysis of Ni/HAP, additional catalytic testing, KIE studies,  
33  
34 DFT calculated gas-phase enthalpies and free energies of reactions, comparison of  
35  
36 TOF values with literature.  
37  
38  
39  
40  
41  
42

## 43 **ACKNOWLEDGEMENTS**

44  
45  
46 This work was funded by Director, Office of Science, Office of Basic Energy  
47  
48 Sciences of the U.S. Department of Energy under Contract No. DE-AC02-05CH11231.  
49  
50 DFT Calculations were performed on a computing cluster sponsored by the National  
51  
52 Institutes of Health (NIH S10OD023532). The authors would like to thank Darinka Primc  
53  
54  
55

for assistance with EDX measurements and Sankaranaryanapillai Shylesh, Neelay Phadke, and Julie Rorrer for helpful discussions.

## REFERENCES

- (1) Roose, P.; Eller, K.; Henkes, E.; Rossbacher, R.; Höke, H. *Amines, Aliphatic*, 5th ed.; Wiley-VCH: Weinheim, 2015.
- (2) Hayes, K. S. Industrial Processes for Manufacturing Amines. *Appl. Catal. A Gen.* **2001**, *221*, 187–195.
- (3) Veefkind, V. A.; Lercher, J. A. On the Elementary Steps of Acid Zeolite Catalyzed Amination of Light Alcohols. *Appl. Catal. A Gen.* **1999**, *181*, 245–255.
- (4) Baiker, A.; Kijenski, J. Catalytic Synthesis of Higher Aliphatic Amines from the Corresponding Alcohols. *Catal. Rev.* **1985**, *27*, 653–697.
- (5) Baiker, A.; Caprez, W.; Holstein, W. L. Catalytic Amination of Aliphatic Alcohols in the Gas and Liquid Phases: Kinetics and Reaction Pathway. *Ind. Eng. Chem. Prod. Res. Dev.* **1983**, *22*, 217–225.
- (6) Corma, A.; Ródenas, T.; Sabater, M. J. A Bifunctional PdVMgO Solid Catalyst for the One-Pot Selective N-Monoalkylation of Amines with Alcohols. *Chem. Eur. J.* **2010**, *16*, 254–260.
- (7) Shimizu, K.; Kon, K.; Onodera, W.; Yamazaki, H.; Kondo, J. N. Heterogeneous Ni Catalyst for Direct Synthesis of Primary Amines from Alcohols and Ammonia. *ACS Catal.* **2012**, *3*, 112–117.
- (8) Rausch, A. K.; van Steen, E.; Roessner, F. New Aspects for Heterogeneous Cobalt-Catalyzed Hydroamination of Ethanol. *J. Catal.* **2008**, *253*, 111–118.
- (9) Sewell, G.; O'Connor, C.; van Steen, E. Reductive Amination of Ethanol with Silica-Supported Cobalt and Nickel Catalysts. *Appl. Catal. A Gen.* **1995**, *125*, 99–112.
- (10) Furukawa, S.; Suzuki, R.; Komatsu, T. Selective Activation of Alcohols in the Presence of Reactive Amines over Intermetallic PdZn: Efficient Catalysis for Alcohol-Based N-Alkylation of Various Amines. *ACS Catal.* **2016**, *6*, 5946–5953.
- (11) Cho, J. H.; Park, J. H.; Chang, T.-S.; Seo, G.; Shin, C.-H. Reductive Amination of 2-Propanol to Monoisopropylamine over Co/ $\gamma$ -Al<sub>2</sub>O<sub>3</sub> Catalysts. *Appl. Catal. A Gen.* **2012**, *417–418*, 313–319.
- (12) Li, S.; Wen, M.; Chen, H.; Ni, Z.; Xu, J.; Shen, J. Amination of Isopropanol to Isopropylamine over a Highly Basic and Active Ni/LaAlSiO Catalyst. *J. Catal.* **2017**, *350*, 141–148.
- (13) Bassili, V. a; Baiker, A. Catalytic Amination of 1-Methoxy-2-Propanol Silica Supported Nickel over Study of the Influence of the Reaction Parameters. *Appl.*

- Catal.* **1990**, *65*, 293–308.
- (14) Fischer, A.; Mallat, T.; Baiker, A. Amination of Diols and Polyols to Acyclic Amines. *Catal. Today* **1997**, *37*, 167–189.
- (15) Šolcová, O.; Jirátová, K. Role of the Support of the Nickel Catalyst in the Synthesis of Morpholine from Diethylene Glycol and Ammonia. *J. Mol. Catal.* **1994**, *88*, 193–203.
- (16) Shimizu, K.; Kanno, S.; Kon, K.; Hakim Siddiki, S. M. A.; Tanaka, H.; Sakata, Y. N-Alkylation of Ammonia and Amines with Alcohols Catalyzed by Ni-Loaded CaSiO<sub>3</sub>. *Catal. Today* **2014**, *232*, 134–138.
- (17) Shimizu, K.; Imaiida, N.; Kon, K.; Hakim Siddiki, S. M. A.; Satsuma, A. Heterogeneous Ni Catalysts for N-Alkylation of Amines with Alcohols. *ACS Catal.* **2013**, *3*, 998–1005.
- (18) Cho, J. H.; An, S. H.; Chang, T. S.; Shin, C. H. Effect of an Alumina Phase on the Reductive Amination of 2-Propanol to Monoisopropylamine over Ni/Al<sub>2</sub>O<sub>3</sub>. *Catal. Letters* **2016**, *146*, 811–819.
- (19) Ho, C. R.; Shylesh, S.; Bell, A. T. Mechanism and Kinetics of Ethanol Coupling to Butanol over Hydroxyapatite. *ACS Catal.* **2016**, *6*, 939–948.
- (20) Tsuchida, T.; Kubo, J.; Yoshioka, T.; Sakuma, S.; Takeguchi, T.; Ueda, W. Reaction of Ethanol over Hydroxyapatite Affected by Ca/P Ratio of Catalyst. *J. Catal.* **2008**, *259*, 183–189.
- (21) Hanspal, S.; Young, Z. D.; Shou, H.; Davis, R. J. Multiproduct Steady-State Isotopic Transient Kinetic Analysis of the Ethanol Coupling Reaction over Hydroxyapatite and Magnesia. *ACS Catal.* **2015**, *5*, 1737–1746.
- (22) Bartholomew, C. H.; Pannell, R. B. The Stoichiometry of Hydrogen and Carbon Monoxide Chemisorption on Alumina- and Silica-Supported Nickel. *J. Catal.* **1980**, *65*, 390–401.
- (23) Shao, Y.; Gan, Z.; Epifanovsky, E.; Gilbert, A. T. B.; Wormit, M.; Kussmann, J.; Lange, A. W.; Behn, A.; Deng, J.; Feng, X.; Ghosh, D.; Goldey, M.; Horn, P. R.; Jacobson, L. D.; Kaliman, I.; Khaliullin, R. Z.; Kus, T.; Landau, A.; Liu, J.; Proynov, E. I.; Rhee, Y. M.; Richard, R. M.; Rohrdanz, M. a.; Steele, R. P.; Sundstrom, E. J.; Woodcock, H. L.; Zimmerman, P. M.; Zuev, D.; Albrecht, B.; Alguire, E.; Austin, B.; Beran, G. J. O.; Bernard, Y. a.; Berquist, E.; Brandhorst, K.; Bravaya, K. B.; Brown, S. T.; Casanova, D.; Chang, C. M.; Chen, Y.; Chien, S. H.; Closser, K. D.; Crittenden, D. L.; Diedenhofen, M.; Distasio, R. a.; Do, H.; Dutoi, A. D.; Edgar, R. G.; Fatehi, S.; Fusti-Molnar, L.; Ghysels, A.; Golubeva-Zadorozhnaya, A.; Gomes, J.; Hanson-Heine, M. W. D.; Harbach, P. H. P.; Hauser, A. W.; Hohenstein, E. G.; Holden, Z. C.; Jagau, T. C.; Ji, H.; Kaduk, B.; Khistyayev, K.; Kim, J.; Kim, J.; King, R. a.; Klunzinger, P.; Kosenkov, D.; Kowalczyk, T.; Krauter, C. M.; Lao, K. U.; Laurent, A. D.; Lawler, K. V.; Levchenko, S. V.; Lin, C. Y.; Liu, F.; Livshits, E.; Lochan, R. C.; Luenser, A.; Manohar, P.; Manzer, S. F.; Mao, S. P.; Mardirossian, N.; Marenich, A. V.; Maurer, S. a.; Mayhall, N. J.; Neuscamman, E.; Oana, C. M.; Olivares-Amaya, R.;

- 1  
2  
3 Oneill, D. P.; Parkhill, J. a.; Perrine, T. M.; Peverati, R.; Prociuk, A.; Rehn, D. R.;  
4 Rosta, E.; Russ, N. J.; Sharada, S. M.; Sharma, S.; Small, D. W.; Sodt, A.; Stein,  
5 T.; Stück, D.; Su, Y. C.; Thom, A. J. W.; Tsuchimochi, T.; Vanovschi, V.; Vogt, L.;  
6 Vydrov, O.; Wang, T.; Watson, M. a.; Wenzel, J.; White, A.; Williams, C. F.; Yang,  
7 J.; Yeganeh, S.; Yost, S. R.; You, Z. Q.; Zhang, I. Y.; Zhang, X.; Zhao, Y.; Brooks,  
8 B. R.; Chan, G. K. L.; Chipman, D. M.; Cramer, C. J.; Goddard, W. a.; Gordon, M.  
9 S.; Hehre, W. J.; Klamt, A.; Schaefer, H. F.; Schmidt, M. W.; Sherrill, C. D.;  
10 Truhlar, D. G.; Warshel, A.; Xu, X.; Aspuru-Guzik, A.; Baer, R.; Bell, A. T.; Besley,  
11 N. a.; Chai, J. Da; Dreuw, A.; Dunietz, B. D.; Furlani, T. R.; Gwaltney, S. R.; Hsu,  
12 C. P.; Jung, Y.; Kong, J.; Lambrecht, D. S.; Liang, W.; Ochsenfeld, C.; Rassolov,  
13 V. a.; Slipchenko, L. V.; Subotnik, J. E.; Van Voorhis, T.; Herbert, J. M.; Krylov, A.  
14 I.; Gill, P. M. W.; Head-Gordon, M. *Advances in Molecular Quantum Chemistry*  
15 *Contained in the Q-Chem 4 Program Package. Mol. Phys.* **2015**, *113*, 184–215.
- 16  
17  
18 (24) Miniach, E.; Śliwak, A.; Moyseowicz, A.; Gryglewicz, G. Growth of Carbon  
19 Nanofibers from Methane on a Hydroxyapatite-Supported Nickel Catalyst. *J.*  
20 *Mater. Sci.* **2016**, *51*, 5367–5376.
- 21  
22 (25) Jun, J. H.; Lee, T. J.; Lim, T. H.; Nam, S. W.; Hong, S. A.; Yoon, K. J. Nickel-  
23 Calcium Phosphate/Hydroxyapatite Catalysts for Partial Oxidation of Methane to  
24 Syngas: Characterization and Activation. *J. Catal.* **2004**, *221*, 178–190.
- 25  
26 (26) Cho, J. H.; Park, J. H.; Chang, T. S.; Kim, J. E.; Shin, C. H. Reductive Amination  
27 of 2-Propanol to Monoisopropylamine over Ni/γ-Al<sub>2</sub>O<sub>3</sub> Catalysts. *Catal. Letters*  
28 **2013**, *143*, 1319–1327.
- 29  
30 (27) Huang, M.; Wang, Q.; Yi, X.; Chu, Y.; Dai, W.; Li, L.; Zheng, A.; Deng, F. Insight  
31 into the Formation of the Tert-Butyl Cation Confined inside H-ZSM-5 Zeolite from  
32 NMR Spectroscopy and DFT Calculations. *Chem. Commun.* **2016**, *52*, 10606–  
33 10608.
- 34  
35 (28) Dumon, A. S.; Wang, T.; Ibañez, J.; Tomer, A.; Yan, Z.; Wischert, R.; Sautet, P.;  
36 Pera-Titus, M.; Michel, C. Direct: N-Octanol Amination by Ammonia on Supported  
37 Ni and Pd Catalysts: Activity Is Enhanced by “Spectator” Ammonia Adsorbates.  
38 *Catal. Sci. Technol.* **2018**, *8*, 611–621.
- 39  
40 (29) Heinen, A. W.; Peters, J. A.; van Bekkum, H. The Reductive Amination of  
41 Benzaldehyde over Pd/C Catalysts: Mechanism and Effect of Carbon  
42 Modifications on the Selectivity. *European J. Org. Chem.* **2000**, No. 13, 2501–  
43 2506.
- 44  
45 (30) Gomez, S.; Peters, J. A.; Maschmeyer, T. The Reductive Animation of Aldehydes  
46 and Ketones and the Hydrogenation of Nitriles: Mechanistic Aspects and  
47 Selectivity Control. *Adv. Synth. Catal.* **2002**, *344*, 1037–1057.
- 48  
49 (31) Verhaak, M. J. F. M.; Dillen, A. J. Van; Geus, J. W. Disproportionation of N-  
50 Propylamine on Supported Nickel Catalysts. *Appl. Catal. A Gen.* **1994**, *109*, 263–  
51 275.
- 52  
53 (32) Shimizu, K. I.; Kon, K.; Shimura, K.; Hakim, S. S. M. a. Acceptor-Free  
54 Dehydrogenation of Secondary Alcohols by Heterogeneous Cooperative Catalysis  
55

- 1  
2  
3 between Ni Nanoparticles and Acid-Base Sites of Alumina Supports. *J. Catal.*  
4 **2013**, *300*, 242–250.  
5
- 6 (33) Cargnello, M.; Doan-Nguyen, V. V. T.; Gordon, T. R.; Diaz, R. E.; Stach, E. a.;  
7 Gorte, R. J.; Fornasiero, P.; Murray, C. B. Control of Metal Nanocrystal Size  
8 Reveals Metal-Support Interface Role for Ceria Catalysts. *Science (80-. )*. **2013**,  
9 *341*, 771–773.  
10
- 11 (34) Kibby, C. L.; Hall, W. Dehydrogenation of Alcohols and Hydrogen Transfer from  
12 Alcohols to Ketones over Hydroxyapatite Catalysts. *J. Catal.* **1973**, *73*, 65–73.  
13
- 14 (35) Natal-Santiago, M. A.; Dumesic, J. A. Microcalorimetric, FTIR, and DFT Studies of  
15 the Adsorption of Methanol, Ethanol, and 2,2,2-Trifluoroethanol on Silica. *J. Catal.*  
16 **1998**, *175*, 252–268.  
17
- 18 (36) Luts, T.; Katz, A. Chemisorption and Dehydration of Ethanol on Silica: Effect of  
19 Temperature on Selectivity. *Top. Catal.* **2012**, *55*, 84–92.  
20
- 21 (37) Barnette, A. L.; Asay, D. B.; Janik, M. J.; Kim, S. H. Adsorption Isotherm and  
22 Orientation of Alcohols on Hydrophilic SiO<sub>2</sub> under Ambient Conditions. *J. Phys.*  
23 *Chem. C* **2009**, *113*, 10632–10641.  
24
- 25 (38) Tsuchida, T.; Sakuma, S.; Takeguchi, T.; Ueda, W. Direct Synthesis of N-Butanol  
26 from Ethanol over Nonstoichiometric Hydroxyapatite. *Ind. Eng. Chem. Res.* **2006**,  
27 *45*, 8634–8642.  
28
- 29 (39) Dobereiner, G. E.; Crabtree, R. H. Dehydrogenation as a Substrate-Activating  
30 Strategy in Homogeneous Transition-Metal Catalysis. *Chem. Rev.* **2010**, *110*,  
31 681–703.  
32
- 33 (40) Almeida, M. L. S.; Beller, M.; Wang, G. Z.; Bäckvall, J. E. Ruthenium(II)-Catalyzed  
34 Oppenauer-Type Oxidation of Secondary Alcohols. *Chem. - A Eur. J.* **1996**, *2*,  
35 1533–1536.  
36
- 37 (41) Ogo, S.; Onda, A.; Iwasa, Y.; Hara, K.; Fukuoka, A.; Yanagisawa, K. 1-Butanol  
38 Synthesis from Ethanol over Strontium Phosphate Hydroxyapatite Catalysts with  
39 Various Sr/P Ratios. *J. Catal.* **2012**, *296*, 24–30.  
40
- 41 (42) Moteki, T.; Flaherty, D. W. Mechanistic Insight to C-C Bond Formation and  
42 Predictive Models for Cascade Reactions among Alcohols on Ca- and Sr-  
43 Hydroxyapatites. *ACS Catal.* **2016**, *6*, 4170–4183.  
44
- 45 (43) Young, Z. D.; Davis, R. J. Hydrogen Transfer Reactions Relevant to Guerbet  
46 Coupling of Alcohols over Hydroxyapatite and Magnesium Oxide Catalysts. *Catal.*  
47 *Sci. Technol.* **2018**, *8*, 1722–1729.  
48
- 49 (44) Cabello, F. M.; Tichit, D.; Coq, B.; Vaccari, A.; Dung, N. T. Hydrogenation of  
50 Acetonitrile on Nickel-Based Catalysts Prepared from Hydrotalcite-like  
51 Precursors. *J. Catal.* **1997**, *167*, 142–152.  
52  
53  
54  
55  
56  
57  
58  
59  
60

## GRAPHICAL ABSTRACT

